JOURNAL OF MATERIALS SCIENCE **35** (2000) 785–793

Tensile creep behavior of 3-D woven Si-Ti-C-O fiber/SiC-based matrix composite with glass sealant

T. OGASAWARA, T. ISHIKAWA, N. SUZUKI
National Aerospace Laboratory (NAL), Mitaka, Tokyo, 181-0015, Japan
E-mail: ogasat@nal.go.jp

I. J. DAVIES
Kyoto Institute of Technology, Sankyo-Ku, Kyoto, 606-8585, Japan

M. SUZUKI
Ube Industries Ltd., Ube, Yamaguchi, 755-8633, Japan

J. GOTOH
Kawasaki Heavy Industries Ltd., Kagamigahara, Gifu, 405-8710, Japan

T. HIROKAWA
Shikibo Ltd., Yokaichi, Shiga, 517-8577, Japan

The present work investigates the tensile creep behavior (deformation and rupture) at 1100–1300 °C in air of a 3-D woven Si-Ti-C-O (Tyranno™) fiber/SiC-based matrix composite with and without glass sealant. The composite contained Si-Ti-C-O fibers with an additional surface modification in order to improve interface properties. Although a significant decrease in tensile strength was observed in the unsealed composite beyond 1000 °C in air (and attributed to oxidation of the fiber/matrix interface), the composite with glass sealant possessed excellent mechanical properties for short-term (<1 hr.) exposure in air. In this study, tensile creep testing was conducted at 1100–1300 °C in air and the effect of glass sealant on medium- and long-term strength was investigated. In addition, chemical stability of the glass sealant was evaluated by X-ray diffraction analysis (XRD) and energy dispersive X-ray spectrometer (EDS). The creep rupture behavior of the composite with glass sealant under long-term exposure is suggested to depend on several factors including decomposition, evaporation, and crystallization of the glass sealant material, in addition to the applied stress.

1. Introduction

Monolithic ceramics typically do not possess the toughness required for aerospace applications. For this reason, significant effort has been devoted to the development of ceramic matrix composites (CMCs) with continuous ceramic fiber reinforcement such as SCS-6™, Nicalon™, and Tyranno™. The National Aerospace Laboratory of Japan, Ube Industries Ltd., Shikibo Ltd., and Kawasaki Heavy Industries Ltd. have conducted a joint program in order to develop and evaluate a ceramic matrix composite. The composite contains Tyranno™ (Si-Ti-C-O) fibers with an additional surface modification in order to improve interface properties. Thus, the fiber/matrix interface is controlled by the heat treatment of the fiber in a carbon monoxide (CO) atmosphere with a SiO_x-rich layer surrounding an inner carbon-rich layer being formed at the fiber surface. Using such technology, the composite exhibits excellent tensile strength (∼400 MPa) at room temperature [1]. However, a significant decrease in tensile strength was observed in the composite beyond 1000 °C in air and this was attributed to oxidation of the fiber/matrix interface and subsequent increase in the fiber debonding shear strength. On the other hand, composite with an additional glass sealant possessed excellent mechanical properties for short-term (<1 hr.) exposure up to 1300 °C in air and in vacuum [2].

In general, the carbon-rich interface layer in SiC/SiC-based composites shows low oxidation resistance at elevated temperature in air [3–5]. The glass sealant for the composite may act as an oxygen diffusion barrier within the composite. A similar phenomenon has been observed in a glass-including matrix Nicalon/SiC-based composite developed by DuPont Lanxide Composites (Wilmington, DE, USA). This composite, termed "enhanced SiC/SiC composite", exhibits excellent strength at 1300 °C in air [6]. In "enhanced SiC/SiC composite", the glass phase in the matrix may seal the matrix cracks at elevated temperature, and prevent oxidation of the fiber/matrix interface.

The present work investigated the tensile creep behavior (deformation and rupture) of the composite at 1100–1300 °C in air. The degradation of glass sealant material after long-term exposure at elevated temperature was also evaluated by a scanning electron microscope (SEM), an energy dispersive X-ray spectrometer (EDS), and an X-ray diffractometer (XRD). The effect of glass sealant on the creep rupture behavior of the composite will be discussed with the experimental results.

2. Experimental procedure

The composite under investigation contained Tyranno^{TM} Lox-M fibers woven into an orthogonal 3-D configuration with fiber volume fractions of 0.19, 0.19, and 0.02 in the x, y, and z directions, respectively. An optical micrograph illustrating the composite fiber architecture has been presented in Fig. 1 with each fiber bundle containing 1600 fibers. The resulting composite preform plate (240 × 120 × 6 mm) was treated at elevated temperature in a CO atmosphere, resulting in formation of a 10 nm SiO_x-rich layer surrounding an inner 40 nm carbon-rich layer at the fiber surface [1]. Polytitanocarbosilane was used as the matrix precursor with repeated impregnation and pyrolysis cycles until satisfactory densification was achieved. The average bulk density of the composite was 2.20 g/cm^2 after machining. Tensile specimens were machined from the composite plates such that the loading direction was parallel to the y-axis. Edge-loaded tensile specimens were used to investigate the monotonic and creep testing. The specimens had 30 mm in gauge length, 4 mm in thickness and width, and 110 mm in the overall length as shown in Fig. 2a. Following machining, tensile specimens were impregnated with a proprietary SiO_2-Na_2O-based water glass. After impregnation of water glass, specimens were treated at elevated temperature. The impregnation process was repeated several times with the aim of improving resistance to oxidation. The weight of the tensile specimen after glass impregnation increased by 4–5%.

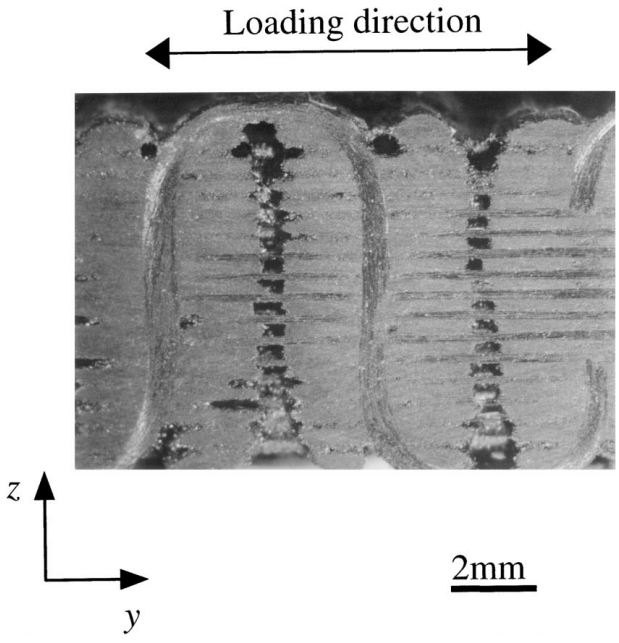

Figure 1 Optical micrograph of Si-Ti-C-O Fiber/SiC-based matrix composite illustrating the 3-D woven fiber configuration (yz plane).

Monotonic tensile and creep testing was conducted on a servo-hydraulic testing system (Model 8501, Instron, USA) at room temperature, 1100 °C, 1200 °C, and 1300 °C in air. The high temperature furnace and contact-type extensometer (Model 2632, Instron, USA) used for these experiments have been shown in Fig. 2b. The gauge length of extensometer was 12.5 mm. Specimens were held for 3 minutes at the test temperature prior to monotonic tensile or creep testing. Monotonic tensile tests were conducted under a constant displacement rate of 0.5 mm/min whilst the time to reach the required stress for creep testing was 3 minutes following holding. The loading rate in creep testing is one of the important test conditions, because microscopic damage during initial loading is strongly influenced by loading rate [7]. As the difference of loading rate for each applied stress was not considerable in the experiment (0.67–1.78 MPa/s) the effect of loading rate on the creep behavior might be negligible.

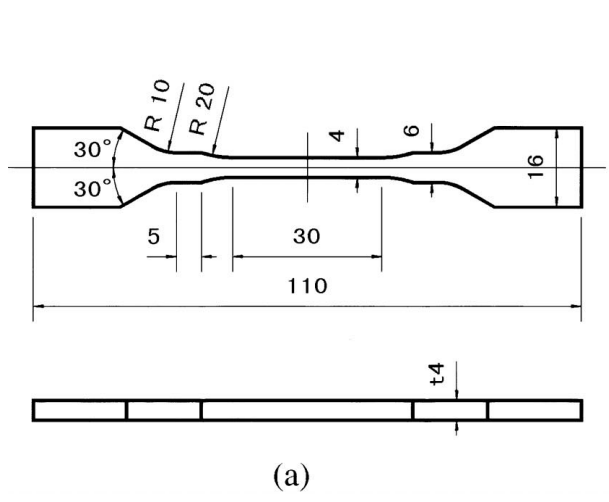

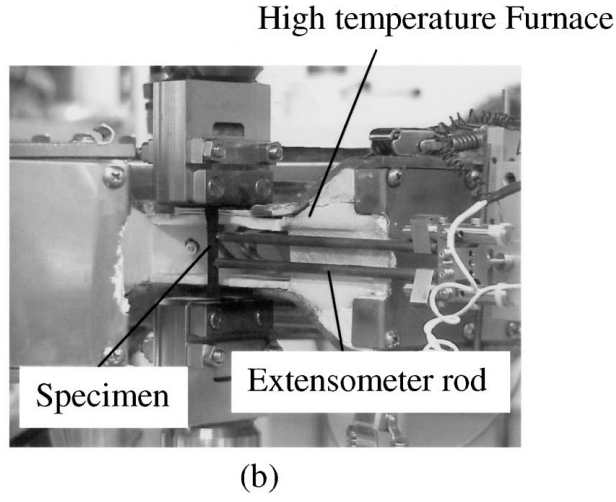

Figure 2 Specimen and test configuration used for monotonic loading and creep testing at elevated temperature: (a) geometry and dimensions of specimen, (b) extensometer and high temperature furnace.

Surface, cross-section, and fracture surface of the specimens were observed using a scanning electron microscope (SEM; Model JSM-6300F, JEOL, Japan and S-4700, Hitachi, Japan). The chemical composition of glass sealant material before and after creep testing was evaluated by energy dispersive X-ray spectrometer (EDS; Model EMAX7000, Horiba, Japan). X-ray diffraction (XRD) analysis was conducted using a Cu-K_α source with X-ray diffractometer (Model RINT2500, Rigaku, Japan) in order to investigate crystallization of the glass phase during creep testing.

3. Results and discussion

3.1. Monotonic tensile behavior

The ultimate tensile strength, S_{UTS}, of specimens as a function of test condition has been presented in Fig. 3. S_{UTS} for unsealed specimens was equivalent at room temperature and 1200 °C in vacuum but decreased rapidly for unsealed specimens tested in air at 1100–1200 °C. The latter trend was attributed to oxidation of the fiber/matrix interface that resulted in a transformation from "pseudo-ductile" to brittle fracture behavior. However, S_{UTS} for specimens tested in air at 1000–1300 °C was significantly improved by the addition of glass sealant, indicating the sealant to protect against oxygen ingression for at least the time scale investigated (on the order of several minutes).

Composite stress-strain curves exhibited an initial linear response followed by non-linear behavior (shown in Fig. 4) for unsealed specimens and sealed specimens in air. However, unsealed specimens showed only the initial linear region prior to failure, suggesting the fibers to have played almost no toughening role in this case and attributed to oxidation of the fiber/matrix interface. The glass sealant material was found to have no significant influence on the composite stiffness, in contrast to the case of "enhanced SiC/SiC composite" [6]. The proportional stress limit, S_{PL}, was approximately 150–170 MPa at elevated temperature. Although matrix cracks in the 0° bundles (y-axis) were thought to occur only above S_{PL}, transverse cracks in the 90° bundles (x and z axis) may well have appeared prior to S_{PL}. As mentioned above, the composite fiber/matrix interface shear strength, τ, was controlled by a thin (40 nm) carbon layer formed by heat treatment of the fiber in a CO atmosphere. Therefore, oxidation of the carbon interface in the unsealed composite would be expected to occur rapidly at elevated temperature in air. The effect of test condition on τ for unsealed and sealed composite has been presented in detail elsewhere [2, 8].

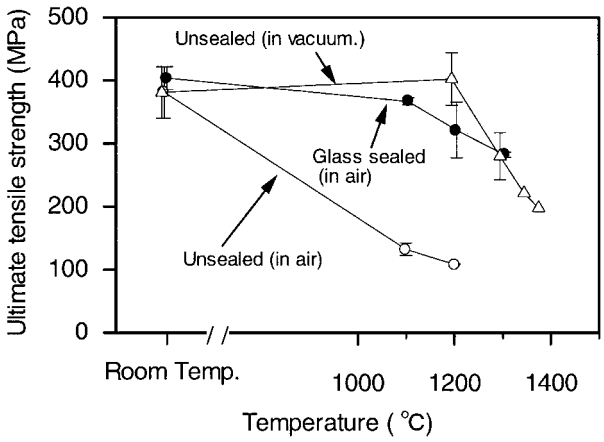

Figure 3 Ultimate tensile strength of the composites tested in vacuum and air at elevated temperature under a constant displacement rate 0.5 mm/min.

3.2. Creep deformation and rupture behavior

Creep rupture data for sealed composite tested at 1100–1300 °C in air has been summarized in Fig. 5. Although the data is seen to have considerable scatter, it would appear that a change in the creep strength degradation behavior occurs in the long-term region at approximately 1×10^6 sec (200–300 hr.) for the 1100 °C case and 3–4 $\times 10^5$ sec (~100 hr.) at 1200 °C. However, this change in creep behavior was not observed at 1300 °C.

The relationship between creep deformation and time at 1200 °C and 1300 °C has been shown in Fig. 6. A quasi-steady state creep region, in which the creep rate was constant, can be observed in both cases. The relationship between applied stress and quasi-steady state creep rate has been presented in Fig. 7. In many case,

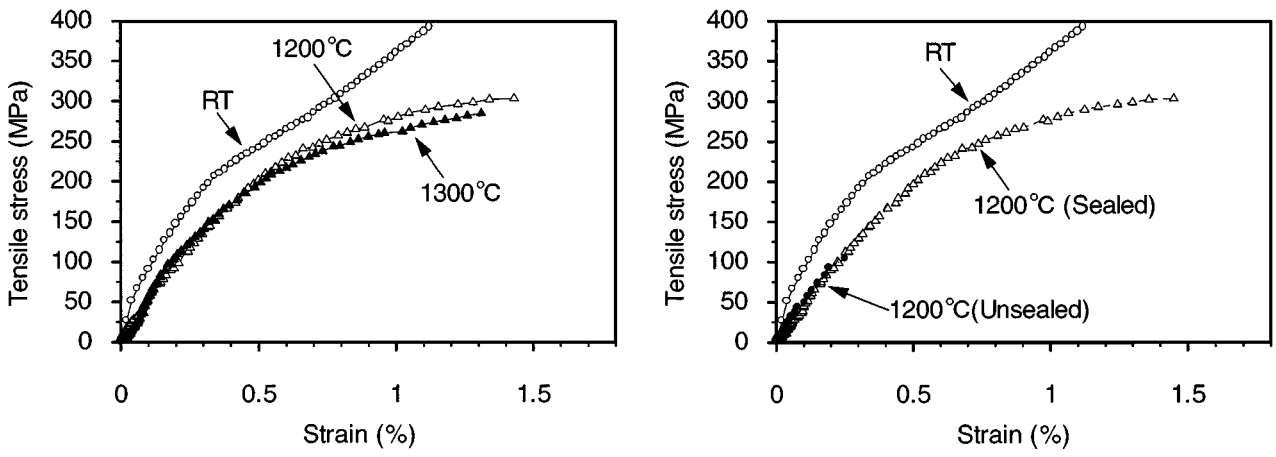

Figure 4 Typical monotonic tensile stress versus strain for sealed and unsealed composite at room temperature, 1200°C and 1300°C in air under a constant displacement rate 0.5 mm/min.

steady state creep rate $\dot{\varepsilon}_{cr}$ under applied creep stress S_c is represented by the following experimental equation.

$$\dot{\varepsilon}_{cr} = AS_c^n \exp\left\{-\frac{Q}{RT}\right\} \quad (1)$$

In the low stress range, the steady state creep rate was found to be insensitive to the applied stress and the stress exponent, n, in this region was 1–2 at both 1100 and 1200 °C whilst the value of n in the higher stress region (>150–170 MPa) was 7–9, again for both cases. Similar results have been reported for SiC-fiber (SCS6)/Si_3N_4 0° composite [9], Nicalon/MLAS 0–90° ply composite [10], and Nicalon/CVI-SiC 0–90° woven composite [11].

The transition stress where the stress exponent changes is believed to correspond to the proportional stress limit S_{PL} (150–170 MPa) in the composite stress-strain curve at elevated temperature (Fig. 4). The stress exponent in the high stress region is also similar to that of "enhanced SiC/SiC composite" reported by Zhu *et al.* [6]. The stress exponent in the low stress region was similar to that for Si-C-O fibers used in previous work [12, 13]. These experimental results indicate that matrix cracks in the 0° bundles have a significant influence on the composite creep deformation. Transverse and matrix cracks that arise during loading at room temperature may be arrested due to the R-curve behavior,

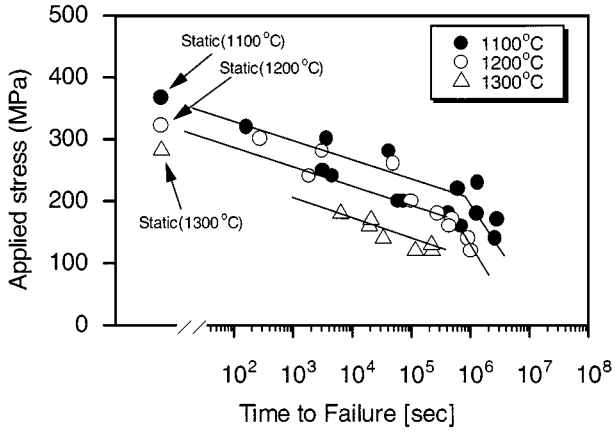

Figure 5 Creep rupture data for sealed composite at 1100°C–1300°C in air.

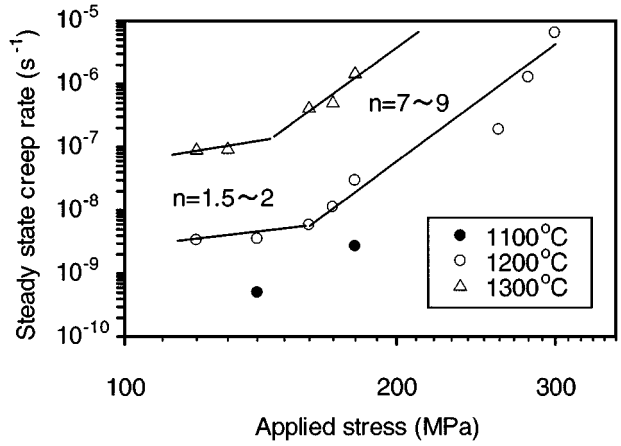

Figure 7 Quasi-steady state creep rate in air versus applied stress for sealed composite at 1100°C–1300°C in air.

i.e., fiber bridging mechanism. However, at high temperature, time-dependent matrix crack growth may take place due to a combination of stress corrosion cracking and creep crack growth of the matrix. The crack opening displacement (COD) contribution from matrix cracks would also be expected to increase due to fiber creep within the matrix cracks. Such slow crack growth and fiber creep increases the specimen compliance and also the steady state creep rate.

SEM micrographs of specimen fracture surfaces following creep testing at 1200 °C have been shown in Fig. 8. It has previously been confirmed by several of the authors that S_{UTS} for this composite is closely predicted by the equation of Curtin [14]:

$$S_{UTS} = V_f S_0^* \left(\frac{2}{m+2}\right)^{\frac{1}{m+1}} \left(\frac{m+1}{m+2}\right) \quad (2)$$

Where S_0^* and m are the *in situ* fiber strength Weibull parameters obtained from fractography studies, and V_f is the fiber volume fraction in the direction of loading. Should all the fibers not be able to contribute to S_{UTS} (for example, due to degradation of the fiber/matrix interface) then V_f should be replaced by the effective fiber volume fraction, V_{eff}. The unsealed composite S_{UTS} at elevated temperature in air is known to be significantly influenced by fiber strength degradation and increased interfacial shear stress [2]. In addition,

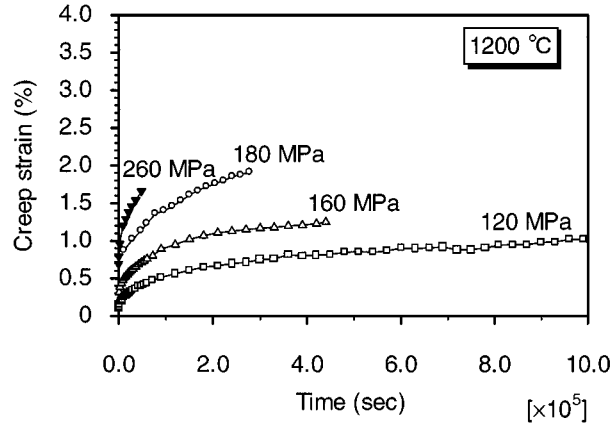

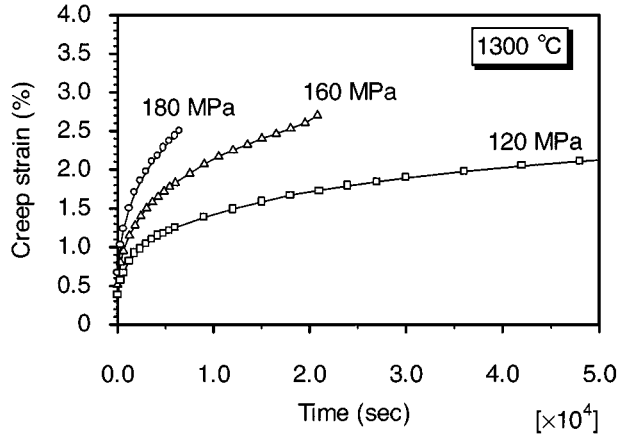

Figure 6 Typical tensile creep strain versus time of the glass sealed composite at 1200°C and 1300°C in air.

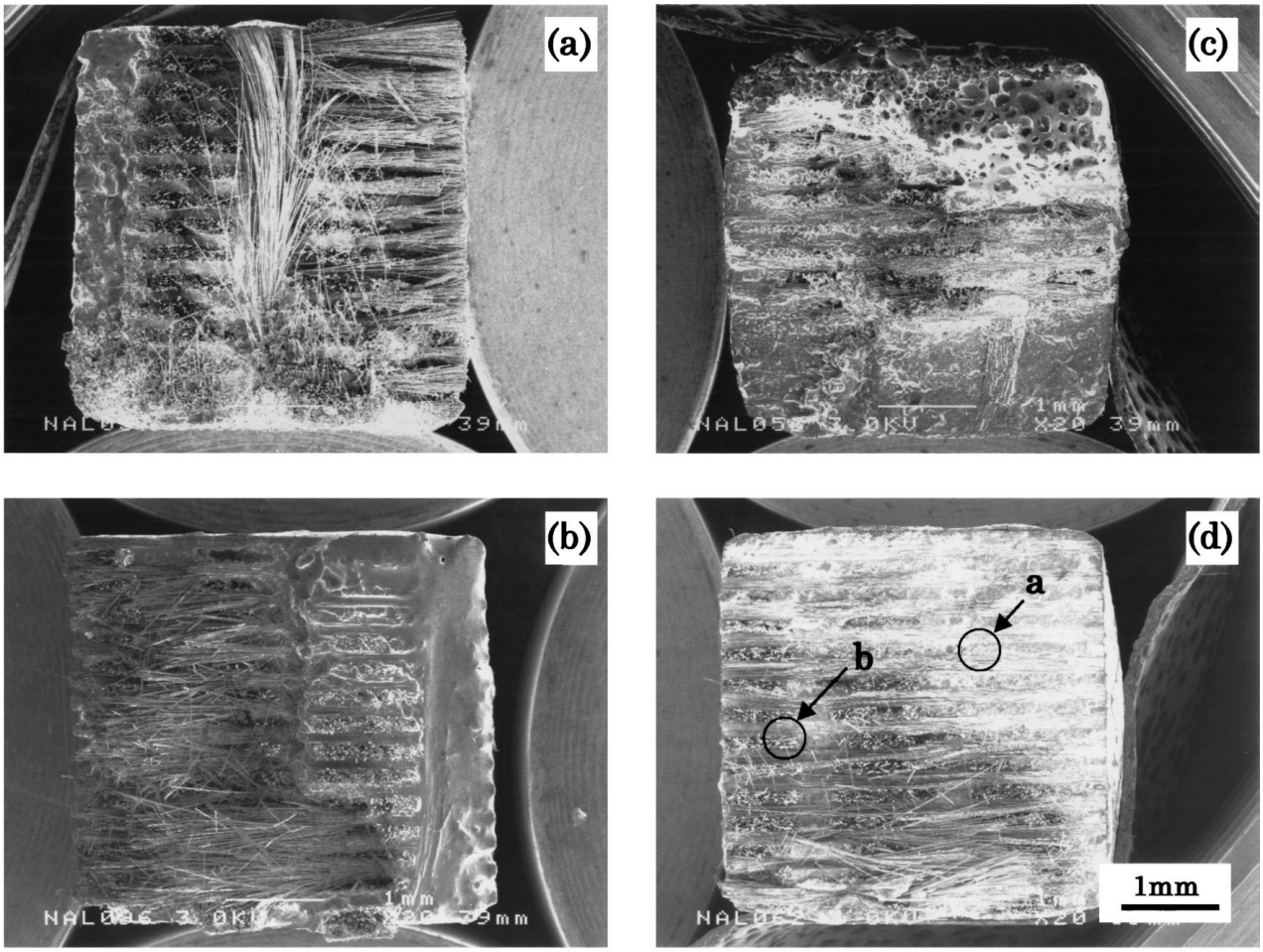

Figure 8 Scanning electron micrographs illustrating fracture surfaces of 3-D woven SiC/SiC based composite after monotonic tensile and creep testing at 1200°C/air:(a) monotonic loading rupture (UTS, 289 MPa), (b) creep rupture (200 MPa, 2080 sec), (c) creep rupture (160 MPa, 4.4×10^5 sec), (d) creep rupture (120 MPa, 1.05×10^6 sec).

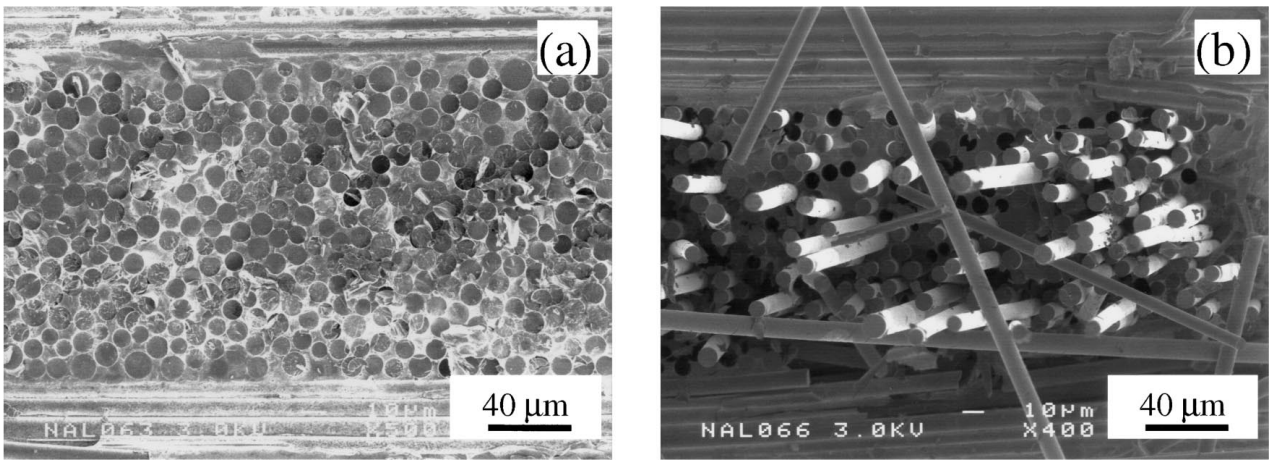

Figure 9 Scanning electron micrographs illustrating fracture surfaces of 3-D woven SiC/SiC based composite after creep testing for 1.05×10^6 sec at 1200°C/air: (a) and (b) are correlated to regions indicated by the arrows shown in Fig. 8d.

increased interfacial shear stress results in the effective fiber fraction being decreased as the number of fibers at which crack deflection takes place is significantly reduced. In effect, the number of fibers that contribute to the composite S_{UTS} decreases with a degradation of fiber/matrix interface properties (i.e., increase in τ).

Fig. 9 presents SEM micrographs taken from two regions in Fig. 8d marked "A" and "B". The micrograph (Fig. 9b) shows a fiber bundle that exhibits significant fiber pullout and hence can be thought of as "effective fibers" that contribute to the composite S_{UTS}. However, Fig. 9a indicates region "A" from Fig. 8d to have a flat fracture surface with negligible fiber pullout. In this case, oxidation of the fiber/matrix interface has increased τ to such an extent that crack deflection did not occur at the fiber/matrix interface–these fibers were thought to have negligible contribution to the composite S_{UTS}.

This phenomenon was investigated further by estimating the size of "oxidized" and "non-oxidized" (i.e., unaffected by oxygen ingression) regions from fracture surface analysis. The resulting data has been presented in Fig. 10 in the form of oxidized region volume fraction, OR_{VF}, as a function of creep stress, S_c. Considering the difficulty in deciding the boundary position between oxidized and non-oxidized regions, a fairly good correlation can be observed in Fig. 10 with OR_{VF} increasing with decreasing S_c. It is clear from this that final composite failure occurs when the remaining "non-oxidized" fibers are not able to sustain the applied creep stress. Linear curve fitting showed S_c to be 384 MPa at $OR_{VF} = 0$ which, again considering the simplistic nature of the calculation, is only ~5% lower than S_{UTS} (404 MPa) at room temperature. Therefore, it may be concluded that those fibers and their interfaces in the unoxidized region should have almost no oxidation damage for short time exposure [8]. If the creep strength of the composite is governed only by oxidized region volume fraction, the creep stress should be equal to $(1 - OR_{VF})S_{UTS}$. However, most of the creep stress data are plotted in lower region of the line $(1 - OR_{VF})$ S_{UTS} as shown in Fig. 10. Therefore, those fibers and their interfaces in the unoxidized region might be damaged for medium- and long-term exposure at elevated temperature in air.

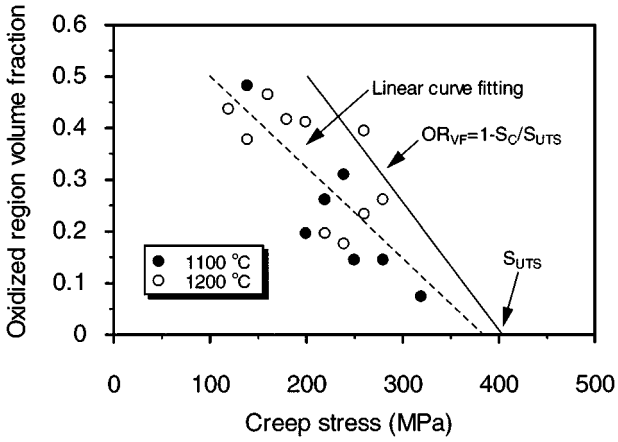

Figure 10 Volume fraction of oxidized region estimated from fracture surface vs. creep stress in air for 3-D woven SiC/SiC-based composite.

3.3. Effect of glass sealant on creep rupture behavior

The effect of glass sealant on mechanical properties of the composite at elevated temperature is significantly important. For long-term exposure at elevated temperature, the degradation of glass sealant material may influence the creep behavior of the composite. SEM micrographs of specimen surfaces prior to and following creep testing at 1200 °C have been shown in Fig. 11. It

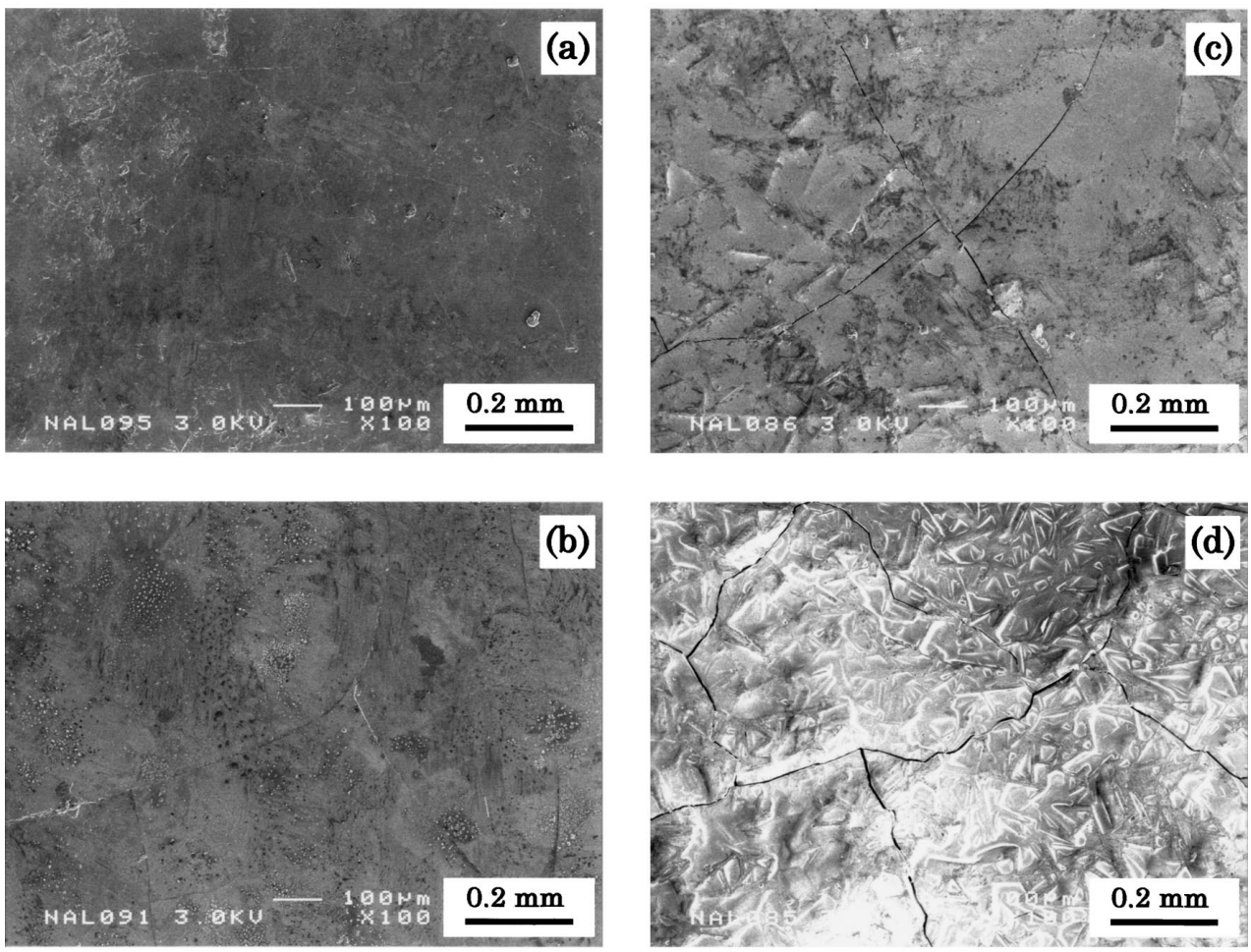

Figure 11 Scanning electron micrographs illustrating the sealed composite surface for 3-D woven SiC/SiC based composite: (a) prior to exposure, and following creep testing at 1200°C/air: (b) 2.08×10^3 sec, (c) 4.4×10^5 sec, (d) 1.05×10^6 sec.

should be noted that these micrographs were taken following cooling and hence may not accurately represent the actual glass sealant surface morphology at elevated temperature. The glass sealant in Fig. 11 is smooth prior to creep testing (Fig. 11a) but becomes progressively rougher with increasing creep time. Figs 11c and d show strong evidence of the presence of crystal structures within the glass sealant and this was confirmed by XRD with data being presented in Fig. 12. From Fig. 12, it is clear that the crystal structure of both fiber and matrix ("unsealed (new)") is polytypic silicon carbide with a very small crystalline size deduced from the relatively broad peak. The sealed specimen prior to creep testing ("sealed (new)") exhibited a small amount of SiO_2 (tridymite) that derived from the glass sealant. The tridymite diffraction peak intensity increased with exposure time and increased rapidly after $3–4\times10^5$ sec (~100 hr.) of exposure. This exposure time corresponds

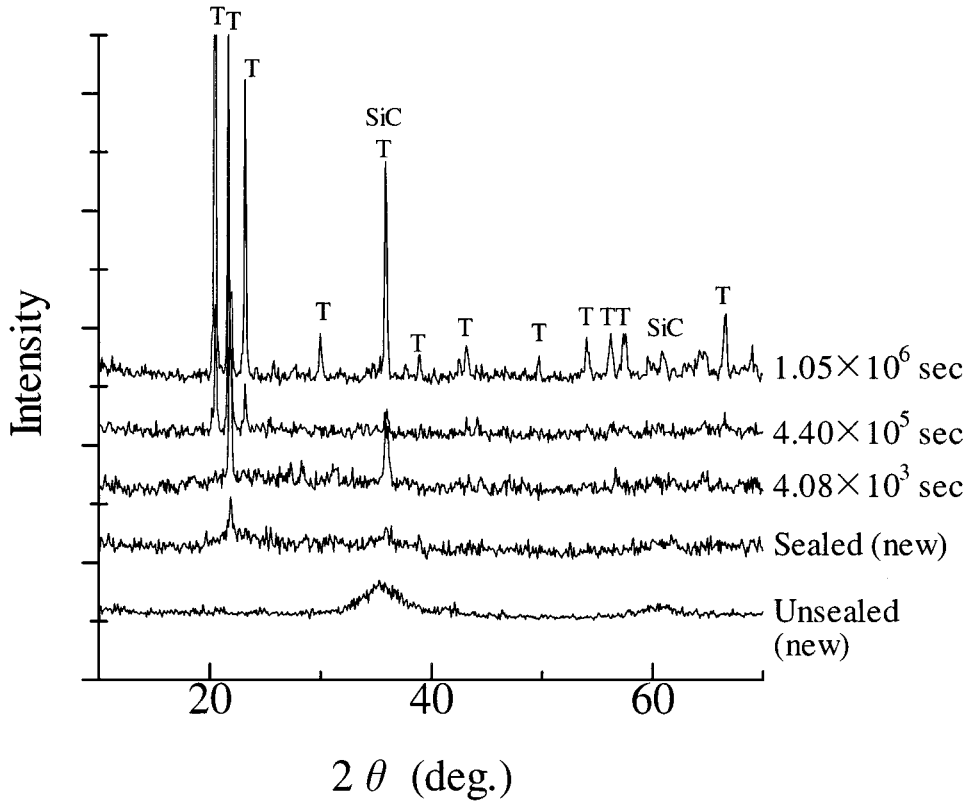

Figure 12 X-ray diffraction (XRD) patterns from the composite surface before and after creep testing at 1200°C in air.

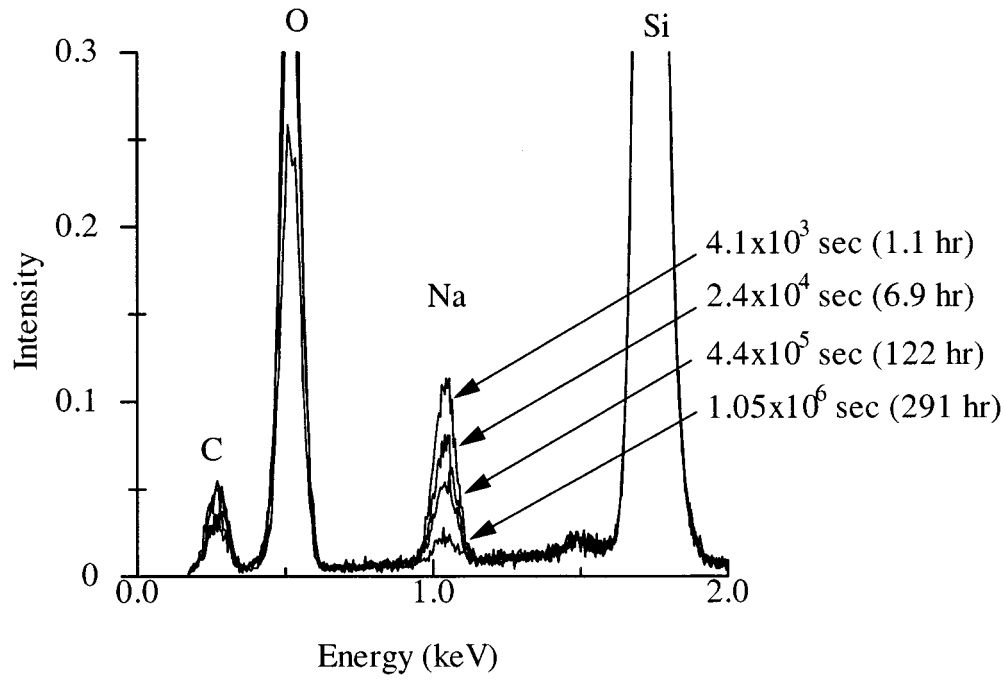

Figure 13 Energy dispersive X-ray spectra (EDS) from specimen surfaces of 3-D woven SiC/SiC based composite after creep testing at 1200°C in air. The spectra are normalized by the peak intensity of silicon.

to the time at which the creep strength decreased significantly (Fig. 5). Therefore, it may be the case that the effectiveness of the glass sealant decreases with increasing crystallinity due to such factors as increased viscosity and volume contraction.

Fig. 13 shows EDS data of the glass sealant after creep testing at 1200 °C. The spectra are normalized by the peak intensity of silicon. Fig. 13 shows clear evidence of the evaporation of sodium (Na), thus, crystallization of glass sealant may be caused by the decomposition during creep testing. SEM observation of fracture surfaces following creep testing showed initial ingression of oxygen into the specimen to occur mainly at the specimen corner (13 out of 17 specimens examined). In three of the remaining specimens, oxygen ingression initiated halfway along the specimen edge at the point where the *z* direction fiber bundle was closest to the specimen surface. The remaining specimen failed due to a large defect within the composite body. Fig. 14a is a SEM micrograph of a specimen that failed after 2.63×10^6 sec exposure to 1100 °C at 140 MPa. Fig. 14b is a schematic representation of the fracture surface showing the expected oxygen path, fiber bundle positions, and boundary between the "oxidized" and "non-oxidized" regions.

One explanation for failure initiation is that the oxidation region may correspond to matrix cracks, i.e., transverse cracks in 90° fiber bundles and matrix cracks

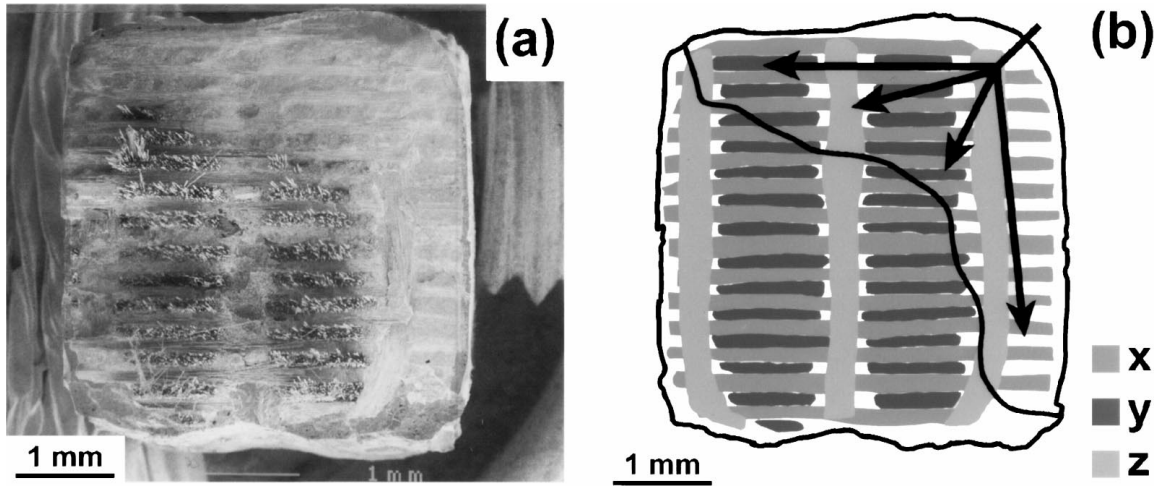

Figure 14 Fracture surface of a 3-D woven SiC/SiC-based composite after creep testing in air (1100°C/140 MPa/2.63×10^6 sec): (a) SEM micrograph, and (b) schematic representation of fracture surface showing fiber bundle positions, oxygen path within composite, and boundary between oxidized and non-oxidized regions.

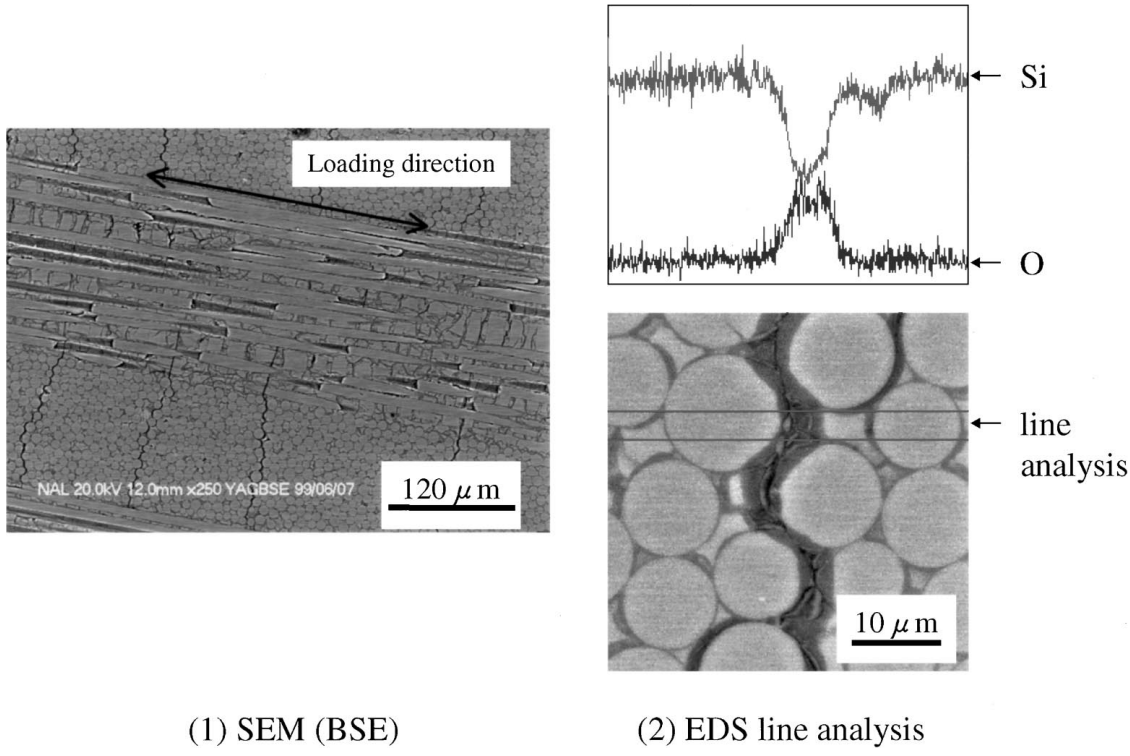

Figure 15 Scanning electron micrograph and EDS line analysis data illustrating the cross section of 3-D woven SiC/SiC based composite after creep testing for 1.05×10^6 sec at 1200°C in air.

in 0° bundles. Glass sealant with a suitably low viscosity to cover the specimen surface and matrix cracks will be effective as an oxygen diffusion barrier. Fig. 15 show the SEM micrograph (back scattering electron (BSE) image) and EDS line analysis data of silicon and oxygen around transverse cracks in the specimen that failed after 1.05×10^6 sec exposure to 1200 °C at 120 MPa. It is revealed that the matrix and fibers adjacent to transverse cracks were strongly oxidized. Oxidation of fibers and matrix can be also observed along matrix cracks in 0° fiber bundles as well as 90° fiber bundles in Fig. 15, therefore, transverse cracks might be oxygen diffusion path in the composite during creep testing.

The glass sealant would cover the specimen surface uniformly and restrict oxygen diffusion into the matrix cracks. At the crack surface and tip, glass sealant impregnated within the composite is also effective as an oxygen diffusion barrier. The size of the oxidation region would be expected to increase with continued loading due to time dependent crack growth factors such as stress corrosion cracking and creep crack growth. Increased viscosity of the glass sealant under long-term exposure, due to the crystallization, would make it difficult for the glass sealant to uniformly cover the composite and crack surface. At this point the glass sealant's function as an oxygen barrier would be degraded. Thus, the creep rupture behavior of the glass sealed composite for long-term exposure would appear to depend not only on the applied stress but also on crystallization of the glass sealant material. Another possible explanation or contributory factor is that it may be easily shown that the glass evaporation rate will increase with decreasing radius of curvature for the specimen surface. Therefore, the maximum glass evaporation rate for these specimens would be at their maximum at the corner regions. Initial differences in glass sealant thickness between the corner and planar regions of the specimen surface also cannot be ruled out.

4. Conclusion

The tensile creep behavior (deformation and rupture) in air at 1100–1300 °C of a 3-D woven Si-Ti-C-O (Tyranno™) fiber/SiC-based matrix composite with glass sealant was investigated. The following conclusions were made:

(1) Although the creep rupture data possessed considerable scatter, the creep strength degradation behavior appeared to change in the long-term region at approximately $1–2 \times 10^6$ sec (200–300 hr.) for specimens tested at 1100 °C, and $3–4 \times 10^5$ sec (∼100 hr.) for those at 1200 °C.

(2) The stress exponent, n, was 7–9 in the high stress region (>150–170 MPa) and 1–2 in the low stress region at both 1100 °C and 1200 °C. The stress exponent in the low stress region was similar (1–2) to that of Si-C-O fibers found in the literature. The transition stress where the stress exponent changed was found to correspond to the proportional limit stress under monotonic tensile loading.

(3) According to XRD analysis of specimen surfaces following creep testing at 1200 °C, crystallization of the glass phase increased rapidly after an exposure time of $3–4 \times 10^5$ sec and this corresponded to the time at which the creep strength significantly decreased.

(4) The creep rupture behavior of the composite with glass sealant under long-term exposure is suggested to depend on a combination of factors such as crystallization of the glass sealant material, specimen geometry, and variations in the glass evaporation rate, in addition to the applied stress.

References

1. T. ISHIKAWA, K. BANSAKU, N. WATANABE, Y. NOMURA, M. SHIBUYA and T. HIROKAWA, *Comp. Sci. Tech.* **58** (1998) 51.
2. I. J. DAVIES, T. ISHIKAWA, M. SHIBUYA, T. HIROKAWA and J. GOTOH, *Composites Part A* **30**(4) (1999) 587.
3. L. FILIPUZZI, G. CAMUS, R. NASLAIN and J. THEBAULT, *J. Amer. Ceram. Soc.* **77**(2) (1994) 459.
4. J. D. CAWLEY, in "Ceramic Transactions, 58: High-Temperature Ceramic-Matrix Composites II," (American Ceramic Society, Westerville, 1995) p. 377.
5. C. F. WINDISCH JR., C. H. HENAGER JR., G. D. SPRINGER and R. H. JONES, *J. Amer. Ceram. Soc.* **80**(3), (1997) 569.
6. S. ZHU, M. MIZUNO, Y. NAGANO, J. CAO, Y. KAGASA and H. KAYA, *ibid.* **81**(9) (1998) 2269.
7. J. W. HOLMES, Y. H. PARK and J. W. JONES, *ibid.* **76**(5) (1993) 1281.
8. I. J. DAVIES, T. ISHIKAWA, M. SHIBUYA and T. HIROKAWA, *Comp. Sci. Technol.* **59**(6) (1999) 801.
9. J. W. HOLMES and XIN WU, in "High Temperature Mechanical Behavior of Ceramic Composites," edited by S. V. Nair and Jakus K. Newton (Butterworth-Heinemann, 1995) 232.
10. H. MAUPAS and J. L. CHERMANT, in "Ceramic Transactions, 57: High-temperature Ceramic-Matrix Composites I," (American Ceramic Society, Westerville, 1995) p. 369.
11. J. CAO, M. MIZUNO and Y. NAGANO, *Ceram. Eng. Sci. Proc.* **19**(3) (1998) 251.
12. R. BODET, X. BOURRAT, J. LAMON and R. NASLAIN, *J. Mater. Sci.* **30** (1995) 661.
13. J. A. DiCARLO, *Comp. Sci. Tech.* **51** (1994) 213.
14. W. A. CURTIN, *J. Amer. Ceram. Soc.* **74**(11) (1991) 2837.

Received 21 June
and accepted 19 August 1999